BOUND STATES OF HEAVY AND LIGHT QUARKS IN THE FRAMEWORK OF QUANTUM CHROMODYNAMICS

By E. J. O. Gavin

Submitted in partial fulfilment of the requirements for the degree of Master of Science in Theoretical Physics at the University of Cape Town

1985

Cape Town

October 1985

Abstract

The spectra of the D, F, B and E mesons have been calculated using the MIT bag model together with a static potential related to the Fourier transform of the "dressed" gluon propagator. The heavy quark has been assumed to coincide with the centre of the bag, while the light antiquark was treated relativistically using the Dirac equation. The spectra obtained are compared with experimental data as well as with the results of other models of these $Q\bar{q}$ mesons. The ratio m_b/m_c obtained in the fit to experimentally known states is compared with the result expected from the hyperfine splitting of the D and B mesons. It appears that this ratio is model dependent. More experimental data are required to further evaluate the validity of this model.

TABLE OF CONTENTS

TABLE OF CONTENTS (continued)

1. Introduction

The term "quarks", first mentioned in James Joyce's esoteric work "Finnegan's Wake" [1], has now become common usage in both "popular" physics, and the less popular variety, such as that appearing in "Physical Review Letters".

Quantum chromodynamics (QCD) is the presently accepted theory of the strong interactions of quarks and gluons. Both are deemed elementary particles, and the constituents of all strongly interacting particles, termed hadrons. Hadrons with integral spin (mesons) are believed to be composed of a quark and antiquark, while those with half-integral spin (baryons) comprise three quarks.

While it is generally believed that the hadronic structure, interactions and spectra can be deduced from QCD, the complexity of this non-abelian gauge theory has led to the deployment of simpler models. Some are based purely on a phenomenological approach; others are to some extent QCD inspired.

The MIT bag model, for example, was developed to describe mesons (and baryons) consisting of light quarks (i.e. up, down and strange), following earlier inadequate non-relativistic approaches. On the other hand, while some models of mesons consisting of heavy quarks have been based on the MIT bag model, the abundant experimental data available on the heavy quarkonium systems (charmonium and bottomium) have largely

been the inspiration for the copious production of non-relativistic potential models, employing a wide variety of potentials.

In contrast, relatively few assays have been made on the mesons consisting of a heavy quark and light antiquark - the mesons resembling the hydrogen atom which contains a heavy proton and light electron.

The description of these mesons in terms of a quark and anti-quark is a two-body problem that requires a relativistic treatment, such as the Bethe-Salpeter equation. If, however, one quark is very heavy, one could treat the motion of the light antiquark using the Dirac equation with an appropriate potential to describe the quark-antiquark interaction - this is the approach adopted here. The interaction of the quark and antiquark is accounted for by a potential derived from QCD. This potential arises from one-gluon-exchange between the quarks, including the corrections arising from vacuum polarisation due to gluon and quark-antiquark pairs.

This potential was derived by R. D. Viollier and J. Rafelski to model charmonium and bottomium [2]. It is not clear that the potential used to describe heavy quark-antiquark systems can be adopted to describe the mesons containing a light quark. Firstly, the Lorentz character of the potential is not well established: by studying the spin splitting of the charmonium states it is possible to conclude that the potential must contain both a Lorentz scalar term, as well as a

term which transforms as the zeroth component of a Lorentz vector. However, the balance between these two contributions, as well as their spatial structure is not certain. Secondly, as the Compton wavelength of the light antiquark is greater that the typical size of a hadron to which the antiquark is confined, the self-energy (or Lamb shift) corrections may be so significant as to render the potential used in modelling heavy quark systems inadequate.

The outline of the report is as follows: first there is an overview of the theoretical framework in Chapter 2. This is followed by the details of the calculation of the meson masses, the gory details of numerical procedures being assigned to an appendix. Next the results of the calculation are presented and compared with the results of previous models of these mesons. The final chapter contains some comments on these results and on the model in general.

Throughout this report the "natural units" of particle physics are employed. The unit system is chosen such that the two fundamental constants of relativistic quantum mechanics, Planck's constant ($\hbar$) and the speed of light in vacuo (c) are one unit of action and one unit of velocity respectively: $\hbar = c = 1$.

2. Theoretical framework

2.1 Quarks, flavour and colour

The existence of quarks was inferred from the fact that the known strongly interacting particles (far too numerous to be classified "elementary" and still please physicists), called hadrons, both bosons (i.e. mesons) and fermions (i.e. baryons), could be grouped in multiplets of particles with similar properties. These multiplets are higher dimensional irreducible representations of the Lie group SU(3). As all higher dimensional representations can be constructed from the fundamental triplet and antitriplet representations of SU(3), it was natural to postulate that the fundamental building blocks of the hadrons were objects that transformed as the fundamental representation of SU(3) [3] .

In this model, the baryons are composed of three quarks (the quark being identified with an SU(3) triplet), while the mesons consisted of a quark and antiquark (an SU(3) anti-triplet). Working out the direct products in terms of irreducible representations one can easily understand why the baryons are grouped in singlets, octets and decuplets:

$$\{3\} \times \{3\} \times \{3\} = \{1\} + \{8\} + \{8\} + \{10\} \qquad (2.1)$$

and the mesons in singlets and octets:

$$\{3\} \times \{\bar{3}\} = \{1\} + \{8\}. \qquad (2.2)$$

Experimental evidence of some substructure to the proton came from the deep inelastic scattering of electrons off protons at

Quark flavour	d	u	s	c	b	t
Electric charge	$-\frac{1}{3}$	$+\frac{2}{3}$	$-\frac{1}{3}$	$+\frac{2}{3}$	$-\frac{1}{3}$	$+\frac{2}{3}$
Third component of isospin	$-\frac{1}{2}$	$+\frac{1}{2}$	0	0	0	0
strangeness	0	0	-1	0	0	0
charm	0	0	0	+1	0	0
bottomness	0	0	0	0	-1	0
topness	0	0	0	0	0	+1

Table 2.1 The six quark flavours and some of their quantum numbers.

SLAC [4] which indicated pointlike, electrically charged objects (termed "partons") within the proton which carried about half the proton's momentum.

As new quark flavours were discovered, the SU(3) symmetry was extended to an SU(N) symmetry (for N quark flavours) and so the original SU(3) multiplets formed submultiplets of the larger SU(N) multiplets. At present six quark flavours are "known", shown in Table 2.1, along with some of their quantum numbers.

Soon after the introduction of quarks, a further degree of freedom was added to this model of hadrons. This was necessary in order to conform with Pauli's exclusion principle which states that the wavefunction describing identical fermions be antisymmetric under interchange of any pair of fermions. For example, in the old picture the spin $\frac{3}{2}$ Δ^{++} resonance consisted of three up quarks, all in the ground state ($l = 0$),

$$|\Delta^{++}, M_z = \tfrac{3}{2}\rangle = |u\uparrow, u\uparrow, u\uparrow\rangle \qquad (2.3)$$

where the $\uparrow$ denotes the projection of the quark spin. This wavefunction is clearly symmetric under the interchange of any two quarks. To antisymmetrise to overall wavefunction, a new quantum number, colour [5], was introduced, such that each quark species could have any one of three colours. The Δ^{++} wave function was thus reinterpreted as

$$|\Delta^{++}, M_z = \tfrac{3}{2}\rangle = \sum_{ijk} \varepsilon^{ijk} |u_i\uparrow, u_j\uparrow, u_k\uparrow\rangle. \qquad (2.4)$$

Later it was realised that this colour degree of freedom was precisely the dynamical concept needed to formulate the theory of the strong interaction [6]. This idea is supported by the fact that leptons which are colourless do not interact strongly, while quarks (now assigned colour) do. As local gauge invariance had provided the basis for understanding the electromagnetic and weak forces, a theory of strong interactions was constructed on the basis of a local colour gauge symmetry. The gauge group chosen was SU(3), a choice governed

by the fact that quarks appeared to be colour triplets. A further indication of the suitability of the symmetry group SU(3) over other symmetry groups such as SO(3) is the fact that it distinguishes between colour and anticolour. This in turn leads to the desirable distinction between quarks and antiquarks: for example, many $q\bar{q}$ states have been observed, while no qq states have yet been found.

2.2 Quantum chromodynamics

The theory of strong interactions obtained by gauging the symmetry group $SU(3)_{colour}$ is known as quantum chromodynamics (QCD). The eight gauge fields describe the gluons which are self-interacting, as this is a nonabelian gauge theory. The gluons are the electrically neutral particles "seen" indirectly in deep inelastic scattering experiments, in that they carry the other half of the proton's momentum.

The Lagrangian density for QCD has the form

$$\mathcal{L}_{QCD} = \bar{\Psi}(x)(i\gamma_\mu \partial^\mu - m)\Psi(x) + g\,\bar{\Psi}(x)\,\gamma_\mu \frac{\vec{\lambda}}{2}\,\Psi(x)\,\vec{A}^\mu(x) - \frac{1}{4}\vec{G}_{\mu\nu}.\vec{G}^{\mu\nu} \qquad (2.5)$$

Here $\Psi(x)$ is the quark spinor and m denotes the mass matrix, the quark masses depending only on flavour. The symbol g stands for the QCD coupling constant. $\vec{\lambda}$ represents the eight 3x3 Gell-Mann matrices ($\frac{\vec{\lambda}}{2}$ are the generators of SU(3)) acting

in colour space. $\vec{A}^{\mu}(x)$ are the eight gauge fields describing the gluons and $\vec{G}^{\mu\nu}$ is the gluon field strength tensor, given by

$$\vec{G}^{\mu\nu} = \partial^{\mu}\vec{A}^{\nu} - \partial^{\nu}\vec{A}^{\mu} + g\,\vec{A}^{\mu} \times \vec{A}^{\nu}. \qquad (2.6)$$

$\mathcal{L}_{QCD}$ is invariant under infinitesimal gauge tranformations of the fields

$$\Psi(x) \rightarrow \Psi'(x) = (1 + i\,\vec{\alpha}(x).\frac{\vec{\lambda}}{2})\,\Psi(x) \qquad (2.7)$$

and

$$\vec{A}^{\mu}(x) \rightarrow \vec{A}^{\mu\prime}(x) = \vec{A}^{\mu}(x) - \frac{1}{g}\,\partial^{\mu}\vec{\alpha}(x) - \vec{\alpha}(x) \times \vec{A}^{\mu}(x). \qquad (2.8)$$

The eight α_k are real phases, which depend on space-time, and the eight-dimensional scalar and vector products are defined as

$$\vec{\alpha}\,.\,\vec{\lambda} = \sum_{k=1}^{8} \alpha_k \lambda_k\,, \qquad (2.9)$$

and

$$(\vec{\alpha} \times \vec{A}^{\mu})_k = \sum_{lm} f_{klm}\,\alpha_l\,A^{\mu}_m \qquad (2.10)$$

respectively, where f_{klm} are the structure constants of SU(3).

The three elementary vertices of QCD are shown in Figure 2.1 , where the first graph (a) describes the two quark - one gluon interaction, the second, (b), corresponds to the three gluon interaction and the third, (c), shows the four gluon interaction.

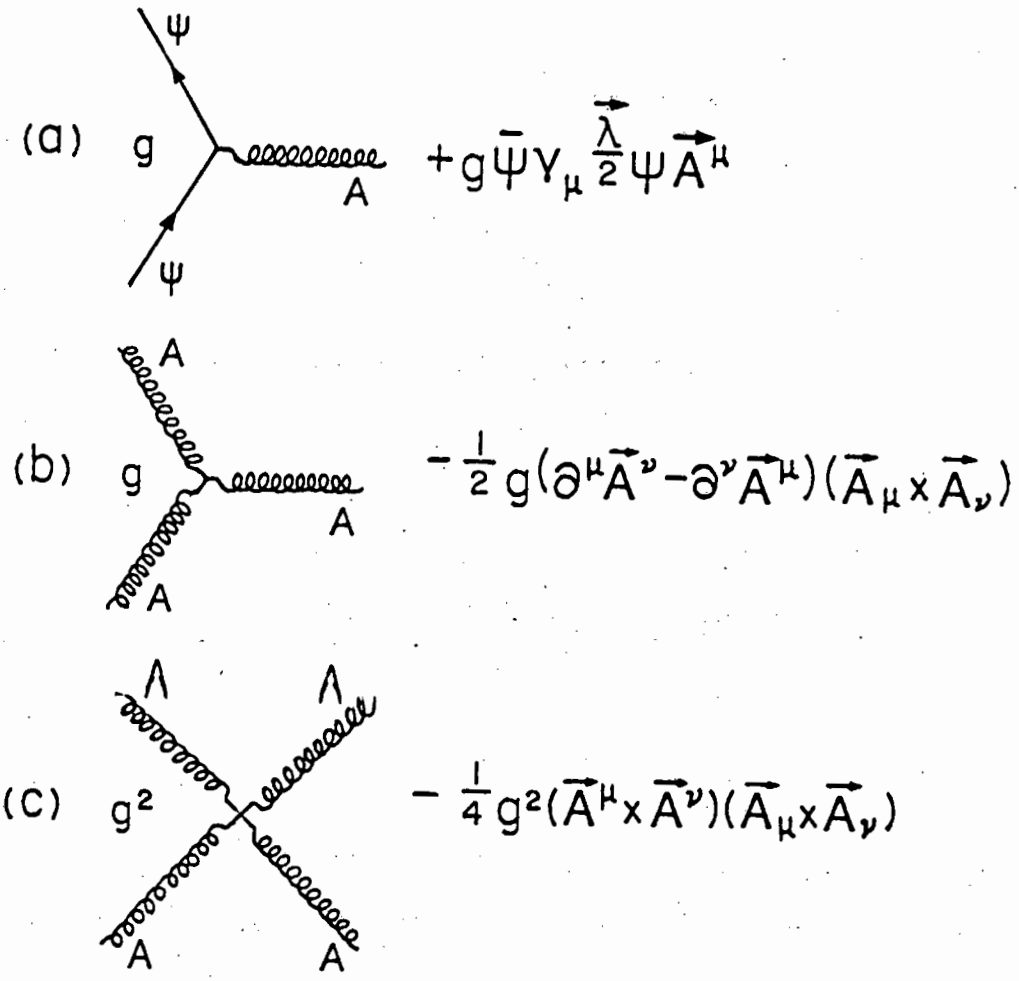

Figure 2.1 The elementary vertices of QCD

The quark-antiquark interaction via one-gluon-exchange is obtained in second order perturbation theory by combining two two quark - one gluon vertices. This interaction is Coulomb like, but higher order perturbations lead to vacuum polarisation corrections which introduce a deviation from this simple form of the potential. The one-loop modifications to the gluon propogator are shown in Figure 2.2.

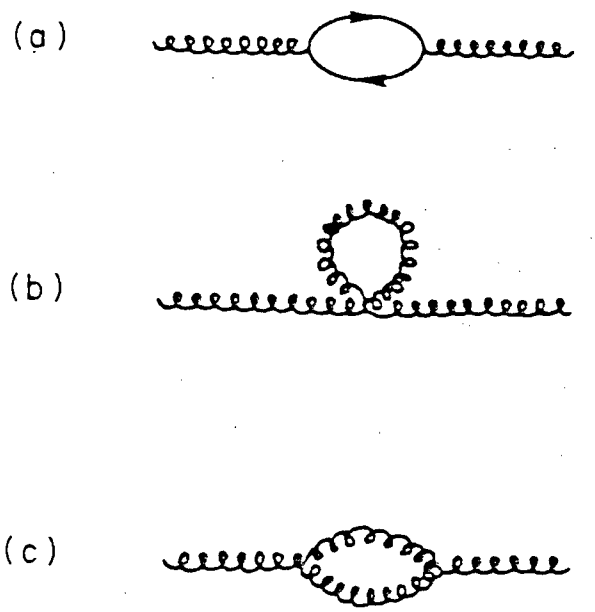

Figure 2.2. One loop modifications to the gluon propogator. (a) is the quark-antiquark loop, (b) the four gluon vertex "tadpole" graph and (c) is the gluon loop.

The Feynman graphs of the one-gluon-exchange form with an arbitrary number of loops can be summed. This series is represented by the running coupling "constant" which depends on the momentum transfer,

$$\alpha_s(q^2) = \frac{12\pi}{(33 - 2f)\log(-q^2/\Lambda^2)} . \qquad (2.11)$$

Here q is the momentum transfer involved in the interaction and f the number of quark flavours in the theory. Λ is a scale parameter which describes the strength of the interaction.

From the form of the running coupling constant, one sees that for $f < 17$, $\alpha_s(q^2)$ becomes small for large q^2, corresponding to small distances, a phenomenon known as asymptotic freedom. This "antiscreening" effect is due to the fact that the gluon loop corrections dominate over the "screening" effect of the quark loop correction to the propagator. This phenomenon supports the use of perturbation techniques in calculations involving large q^2.

It can also be seen that $\alpha_s(q^2)$ increases with increasing q^2, or, correspondingly, at large distances. This phenomenon of stronger attraction with increasing separation of quarks lends some support to the idea that colour and consequently coloured objects are confined. While it is believed that colour confinement is a consequence of QCD, this has not been shown rigorously. Postulating that only colour singlets are observable explains the non-observation of free quarks, as well as why only certain combinations of quarks and antiquarks have been seen. One can construct a colour singlet state by combining 3n colour triplets and/or any number of triplet - antitriplet pairs, similar to $SU(3)_{flavour}$ (see equations (2.1) and (2.2)).

2.3 The MIT bag model

In the MIT model [7], a modified Lagrange density is introduced in order to incorporate confinement phenomenologically

$$\mathcal{L}_{bag} = (\mathcal{L}_{QCD} - B)\,\Theta_s(x) - \frac{1}{2}\bar{\psi}\psi\,\delta_s(x). \qquad (2.12)$$

B is known as the vacuum pressure. $\Theta_s(x)$ is a step function, equal to 1 inside the bag, and 0 outside. δ_s is a surface delta function, defined as

$$\delta_s(x) = n_\mu \partial^\mu \Theta_s(x)\ . \qquad (2.13)$$

where $n_\mu = \{n_0, -\vec{n}\}$ is a spacelike unit vector with $\vec{n}$ perpendicular to the bag surface and pointing outwards.

In this approach, confinement is incorporated by imposing boundary conditions on the quark and gluon fields at the surface of a cavity. Within this cavity, the short-range interactions of the quarks and gluons can be treated in perturbation theory. This region is consequently known as the perturbative vacuum, while the region outside the bag or cavity is termed the real or perturbative vacuum.

Solving the Dirac equation for the quark fields $\Psi(r)$ subject to the linear bag boundary condition

$$-i\vec{n}.\vec{\gamma}\,\Psi(r) = \Psi(r) \qquad (2.14)$$

completely determines the allowed cavity modes and the total energy of the quarks E_q. The quadratic boundary condition requires that the Dirac pressure of the quarks and Maxwell

pressure of the gluons be balanced by the vacuum pressure. In the case of a static, spherical surface, this condition amounts to the minimisation of the energy with respect to the confinement radius. The total energy $E(r_b)$ of a hadron containing n quarks is given by

$$E(r_b) = \sum_{i=1}^{n} E_i(r_b) + Z_0/r_b + B \frac{4}{3} \pi r_b^3 \qquad (2.15)$$

E_i is the energy of the i^{th} quark. Z_0/r_b is the "zero-point" energy term, which includes the Casimir effect and the centre-of-mass energy. The mass of the hadron is obtained by minimising expression (2.15) with respect to the confinement radius r_b.

2.4 Potential models

Another approach in the modelling of hadrons, in particular the known heavy quarkonium systems (J/Ψ and Υ), has been that of potential models, especially non-relativistic potential models. The interaction of the quarks is described by a potential term in the Schrodinger equation which is then solved to give the eigen modes of the quarks. The potential chosen includes some kind of monotonically rising function of the distance between the quarks, which implements the confinement of the hadronic constituents.

Many such potentials have been used, but two of these are specifically mentioned below, as they have been used in modelling $Q\bar{q}$ systems.

2.4.1 The Cornell Potential

In a non-relativistic treatment, Eichten et al. [8] obtained estimates of the masses of $Q\bar{q}$ systems. They used a linear plus Coulomb potential (known as the Cornell potential)

$$V(r) = -\frac{k}{r} + \frac{r}{a} \quad , \tag{2.16}$$

where k and a are constants to describe the spin-independant interaction of the quark and antiquark. Corrections due to spin-orbit and hyperfine interactions were based on the experimental data available on the K mesons together scaling arguments.

2.4.2 The Richardson potential

Richardson developed a potential that incorporated both asymptotic freedom and confinement [9],

$$V(r) = \frac{8\pi}{33-2f}\,\Lambda\left(\Lambda r - \frac{f(\Lambda r)}{\Lambda r}\right) \tag{2.17}$$

where

$$f(t) = \frac{4}{\pi}\int_1^{\infty} dq\,\frac{\sin(qt)}{qt}\left[\frac{1}{\ln(1+q^2)} - \frac{1}{q^2}\right] \tag{2.18}$$

This potential was employed by Crater and van Alstein in a consistent relativistic, two-body formulation [10] to obtain the mass spectra of the $Q\bar{q}$ systems. They treated the confining part of the potential as a Lorentz scalar and the modified Coulomb term as the zeroth component of a Lorentz vector.

3. Calculation of the mass of the $Q\bar{q}$ system

Mesons consisting of a heavy quark Q (i.e. charm or bottom) and a light antiquark $\bar{q}$ (i.e. up, down or strange), or a heavy antiquark and a light quark, can be described within the framework of the MIT bag model. The Dirac equation, together with the linear bag boundary condition, determines the wavefunction and energy eigenvalue of the light antiquark. In contrast to the usual MIT bag model, the cavity modes are not the solutions of the free Dirac equation, as the interaction of the heavy quark with the light antiquark is described by a static potential.

The heavy quark is regarded as infinitely heavy and so coincides with the origin of both the static, spherically symmetric potential and the bag within which the light antiquark moves. In this limit, the problems and ambiguities arising in the reduction of a relativistic two-body equation to a one-body equation using some sort of "reduced mass" and "effective energy" co-ordinates are avoided [11].

The mass of the $Q\bar{q}$ system is then calculated as follows. First the energy of the light antiquark $E_q(r_b)$ is obtained by solving the Dirac equation with the static potential, subject to the linear bag boundary condition. The energy E of the $Q\bar{q}$ system, as a function of the confinement radius r_b, is then given by

$$E(r_b) = m_Q + E_q(r_b) + B\,\frac{4}{3}\,\pi\, r_b^3 , \qquad (3.1)$$

where m_Q is the mass of the heavy quark and B the MIT bag pressure. The absence of a "zero point" energy term is consistent with other models which use the MIT bag framework to describe hadrons containing a heavy quark [12].

The single particle energy E_q and the volume energy term both depend on the radius of confinement: E_q decreases as r_b increases and the volume term increases with increasing r_b. In the absence of a $\bar{Q}q$ potential, E_q scales as r_b^{-1} for a massless antiquark. With an additional potential, the scaling law is not as simple, but E_q is nevertheless a decreasing function of r_b for reasonable values of the confinement radius (i.e. for $r_b > 0.2$ fm). The mass M of the $\bar{Q}q$ meson is thus obtained by minimising $E(r_b)$ with respect to r_b

$$M = \min E(r_b). \qquad (3.2)$$

3.1 Solution of the Dirac equation in spherical co-ordinates

The energy eigenvalue E_q of the light antiquark is obtained by solving the time-independent Dirac equation

$$\{-i\,\vec{\alpha}.\vec{\nabla} + \beta m_q + \beta S(r) + V(r)\}\Psi(r) = E_q \Psi(r), \qquad (3.3)$$

where m_q is the quark mass, S(r) is a potential that transforms as a Lorentz scalar and V(r) is a potential that transforms as the zeroth component of a Lorentz vector.

As both these potentials are spherically symmetric, it is convenient to solve the Dirac equation in spherical coordinates. The four-component Dirac wave function Ψ can be written in the form

$$\Psi = \begin{pmatrix} g_{n,K}(r)\ \chi^{M}_{K}(\hat{r}) \\ i f_{n,K}(r)\ \chi^{M}_{-K}(\hat{r}) \end{pmatrix} , \tag{3.4}$$

where $g_{n,K}(r)$ and $f_{n,K}(r)$ denote the large and small components respectively, and $\chi^{M}_{K}(\hat{r})$ are the usual spherical spinors.

Dirac's quantum number, K, is related to the total angular momentum j and the orbital angular momenta of the large and small components (l and $\bar{l}$ respectively) by

$$\begin{aligned} j(K) &= |K| - \tfrac{1}{2} , \\ l(K) &= j + \tfrac{1}{2} \operatorname{sgn} K, \\ \bar{l}(K) &= j - \tfrac{1}{2} \operatorname{sgn} K. \end{aligned} \tag{3.5}$$

Inserting (3.4) into (3.3) one obtains the following coupled first order differential equations for the radial part of the wave function [13]:

$$\frac{df}{dr} = \frac{K-1}{r} f - (E_q - V(r) - m_q - S(r)) g \qquad (3.6)$$

$$\frac{dg}{dr} = (E_q - V(r) + m_q + S(r)) f + \frac{-K-1}{r} g \; . \qquad (3.7)$$

3.2 Potentials used in the model

The interaction of the quark and antiquark is here described by the exchange of one gluon, taking vacuum polarisation into account. The one-gluon-exchange leads to a Coulomb-like potential which is then modified by the vacuum polarisation contribution due to gluon and light quark-antiquark pairs. Thus the quark-antiquark potential is related to the Fourier transform of the dressed gluon propogator [14]:

$$V(r) = \begin{cases} -\dfrac{4}{3B_f r} \displaystyle\int_0^\infty \dfrac{(1 - \exp(-Mr)]\, dM^2}{[(\log(M^2/\Lambda^2)^2 + \pi^2]\, M^2} & \text{for } r < r_b \\ V(r_b) & \text{for } r > r_b \end{cases} \qquad (3.8)$$

where

$$B_f = (33 - 2f)/12\pi \; . \qquad (3.9)$$

Here f is the number of quark flavours contributing to the polarizability of the vacuum and Λ is a mass scale parameter which governs the strength of the interaction.

The three lightest quarks will contribute significantly to the polarizability of the perturbative vacuum. One can take the up and down quarks as massless, but must allow for a finite mass of the strange quark, m_s. Each quark flavour contributes to the vacuum polarisation for distances corresponding to $(2 m_q)^{-1}$ or less. To interpolate smoothly between the two cases where only the up and down quarks contribute ($f = 2$) and where the strange quark contributes too ($f = 3$), the constant B_f in equation (3.8) is replaced by $B_{eff}(r)$ [15] given by

$$\frac{1}{B_{eff}(r)} = \frac{1}{B_2} + \left(\frac{1}{B_3} - \frac{1}{B_2} \right) (\exp(-2 m_s r) \qquad (3.10)$$

The exchange potential, shown in Figure 3.1, is assumed to transform as the zeroth component of a Lorentz vector and so cannot provide confinement.*) To ensure confinement a scalar potential which is equivalent to the linear boundary condition of the MIT bag model must is introduced:

$$S(r) = \begin{cases} 0 & \text{for } r < r_b \\ S_0 & \text{for } r > r_b \end{cases}, \text{ with } S_0 \to \infty. \qquad (3.11)$$

*) Also, neither a scalar nor vector 1/r potential can bind a massless Dirac particle [16].

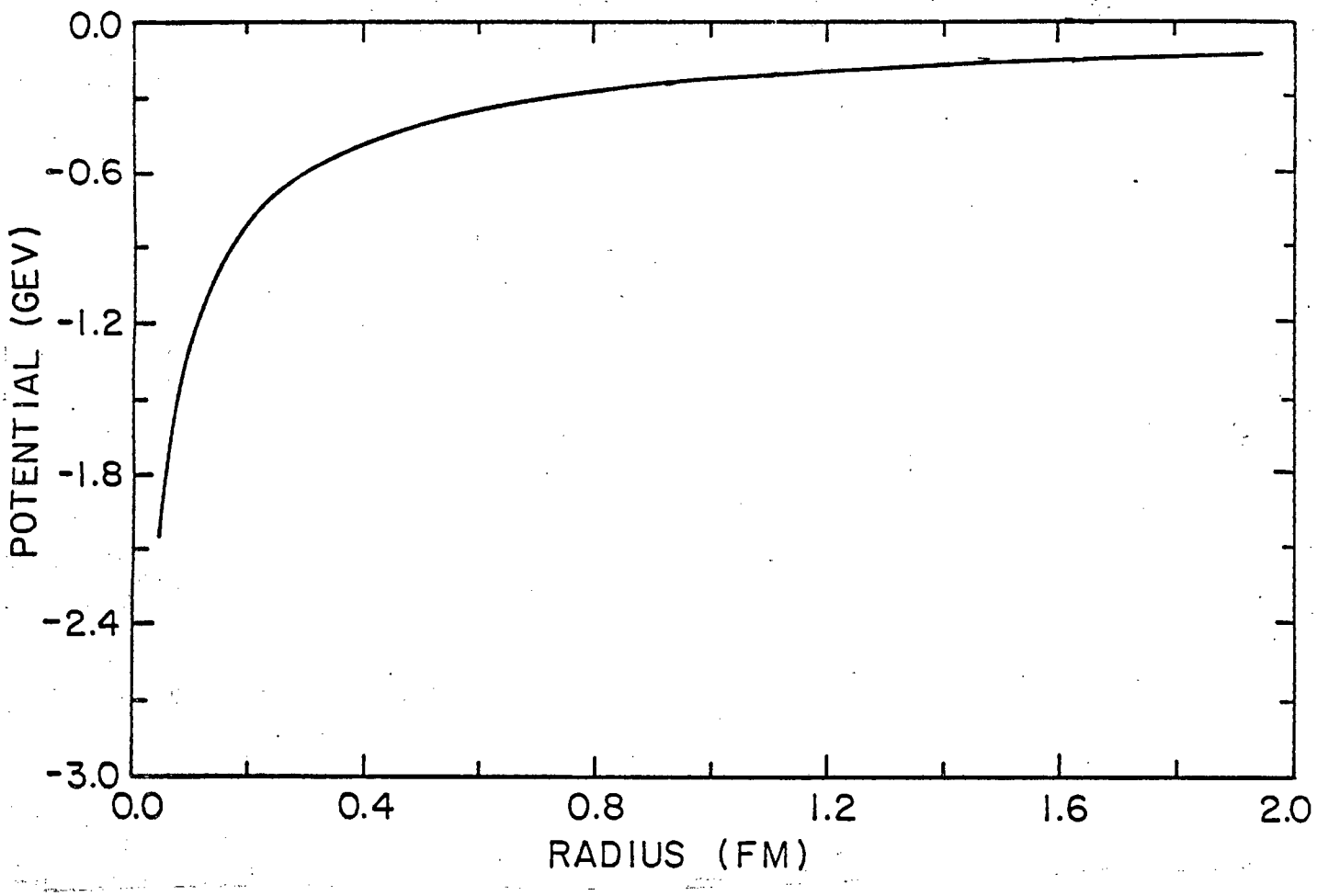

Figure 3.1 The exchange potential

3.3 Bound state solutions of the Dirac equation

Where equations (3.6) and (3.7) cannot be solved analytically (as is the case for the potential described in Section 3.2), they must be integrated numerically to obtain the wavefunction (see Appendix A, Section A.3).

The equations for f and g are integrated numerically from the origin towards the confinement radius and from outside the bag towards the boundary. For the numerical integration, the initial values of the wavefunctions must be supplied. The initial conditions must be determined so that the bound state

wave function is regular both at the origin and at infinity to ensure the square integrability of the wave function. Manipulating equations (3.6) and (3.7) for V(r) = V and S(r) = S (V and S constants) one obtains the following second order differential equations containing g or f only:

$$r^2 \frac{d^2g}{dr^2} + 2r \frac{dg}{dr} + \{(pr)^2 - K(K+1)\}\, g = 0 \qquad (3.12)$$

$$r^2 \frac{d^2f}{dr^2} + 2r \frac{df}{dr} + \{(pr)^2 - K(K-1)\}\, f = 0 \,. \qquad (3.13)$$

The solutions of these equations are a linear combination of spherical Bessel functions of argument pr, where

$$p^2 = (E_q - V)^2 - (m_q + S)^2 . \qquad (3.14)$$

Setting the initial values of g and f outside the scalar potential well presents no difficulty as V(r) and S(r) are both constants. The functions g and f must be finite at infinity, so they are set as

$$g(r_o) = h_l^{(1)}(pr_o) \qquad (3.15)$$

and

$$f(r_o) = \frac{\mathrm{sgn}(K)\, p}{E_q - V(r_b) + m_q + S_0} h_{\bar{l}}^{(1)}(pr_o) \qquad (3.16)$$

where r_o is the value of r at which the inward integration begins, and $h_n^{(1)}$ denotes the spherical Hankl function of the first kind, of order n.

Inside the potential well, while S(r) is constant (zero), V(r) is not. In order to define the initial values of g and f for the integration, V(r) is "cut off" at $r = r_i$, i.e. set to $V(r_i)$ for $r < r_i$, where r_i is the initial value of r for the outward integration. This initial value for r must be sufficiently small so that it does not strongly affect the behaviour of the wavefunctions obtained in the numerical integration.

For $p^2 > 0$ at r_i, f and g must be spherical Bessel functions of the first kind,

$$g(r_i) = j_l(pr_i) \tag{3.17}$$

and

$$f(r_i) = \frac{\mathrm{sgn}(K)\, p}{E_q - V(r_i) + m_q} j_{\bar{l}}(pr_i) \tag{3.18}$$

as these are the only solutions that are regular at the origin.

When $p^2 < 0$, f and g are set to the only combination of Hankl functions regular at the origin, $h^{(1)}_K + h^{(2)}_K$ *). Thus

$$g(r_i) = h^{(1)}_l(pr_i) + h^{(2)}_l(pr_i) \tag{3.19}$$

and

$$f(r_i) = \frac{\mathrm{sgn}(K)\, p}{E_q - V(r_i) + m_q} \{h^{(1)}_{\bar{l}}(pr_i) + h^{(2)}_{\bar{l}}(pr_i)\}. \tag{3.20}$$

*) Bound state solutions in this region would give SLAC bag-like probability of finding the quark in a region peaked sharply around the bag boundary [17].

Both the large and small component of the Dirac wavefunction must be continuous at all points in space, in particular at the boundary. It is this constraint which determines the allowed energies of the quark: only for certain values of the energy can regular solutions of both the upper and lower component be matched simultaneously at the boundary. This condition is equivalent to the linear boundary condition of the MIT bag model in the limit where the scalar step potential becomes infinite (this is shown in Appendix B).

4. Results

4.1 Single particle energies states as a function of the potential strength

The single particle energies of a light antiquark moving in the one-gluon exchange potential are shown in Figure 4.1. The energy eigenvalues of the various states are plotted as a function of the strength of the interaction in the case of a massless quark in Figure 4.1(a) and in Figure 4.1(b) for a quark with mass 0.3 GeV which corresponds to the approximate value of the strange quark mass in this model. The positive energy solutions for a given K are labelled by n = 1,2,... with increasing energy while the negative energy solutions are indexed by n = -1,-2,... with decreasing energy.

As expected for a potential which transforms as the zeroth component of a four-vector, the energy of both the positive and negative energy states decreases as a function of the strength of the potential. It is also clear that the states with higher angular momentum are less influenced by the one-gluon-exchange potential than the lower angular momentum states. This is due to the centrifugal barrier which leads to the repulsion of states with higher angular momentum away from the origin. In the case of the lower angular momentum states, there is a slight but noticable deviation from the linear dependence of the energy of the states on the potential strength which would be expected from first order perturbation theory. In the limit of vanishing vector potential which

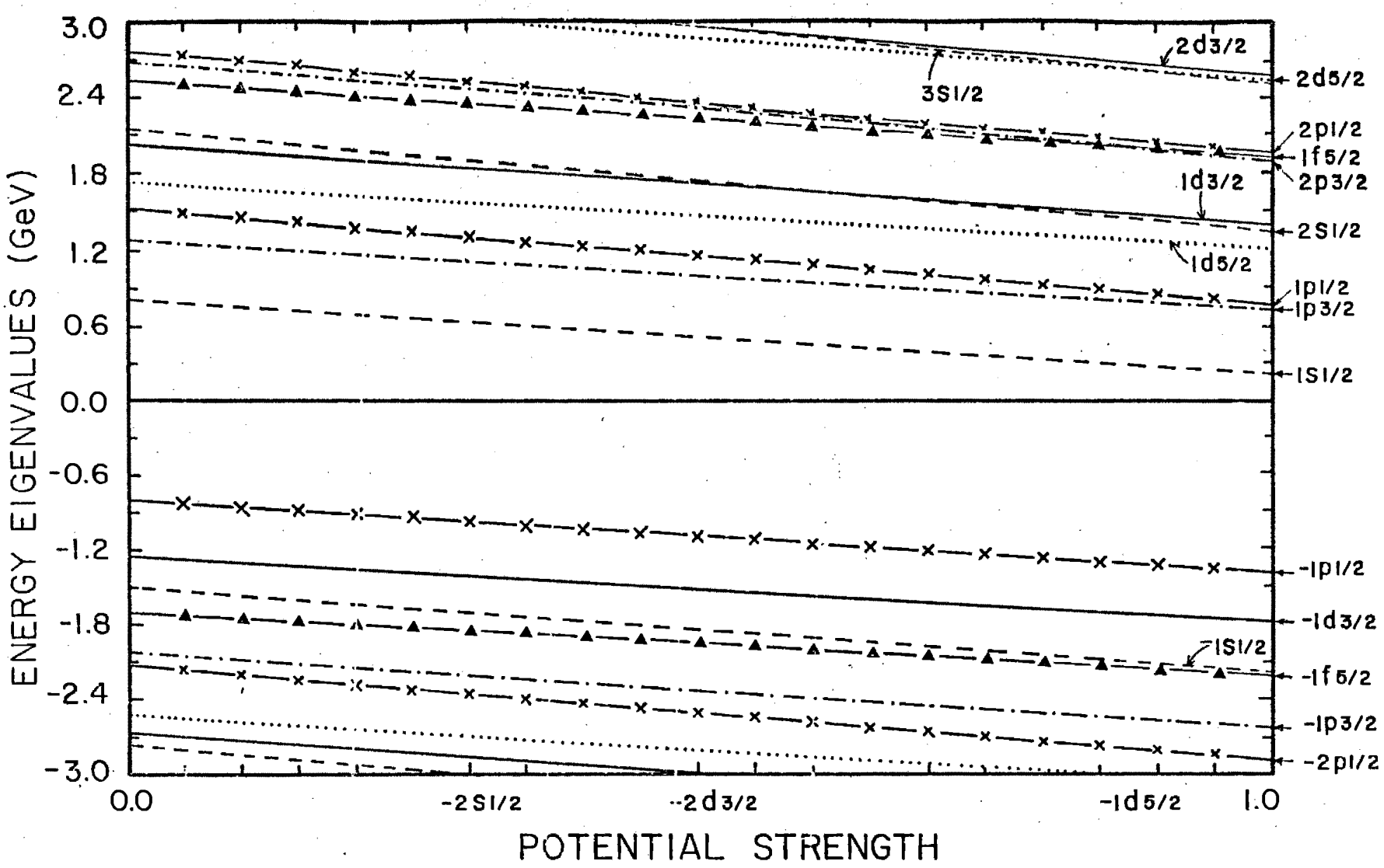

Figure 4.1 (a). The single particle energy as a function of potential strength for a massless antiquark. The full value of the potential used in this model is on the extreme right

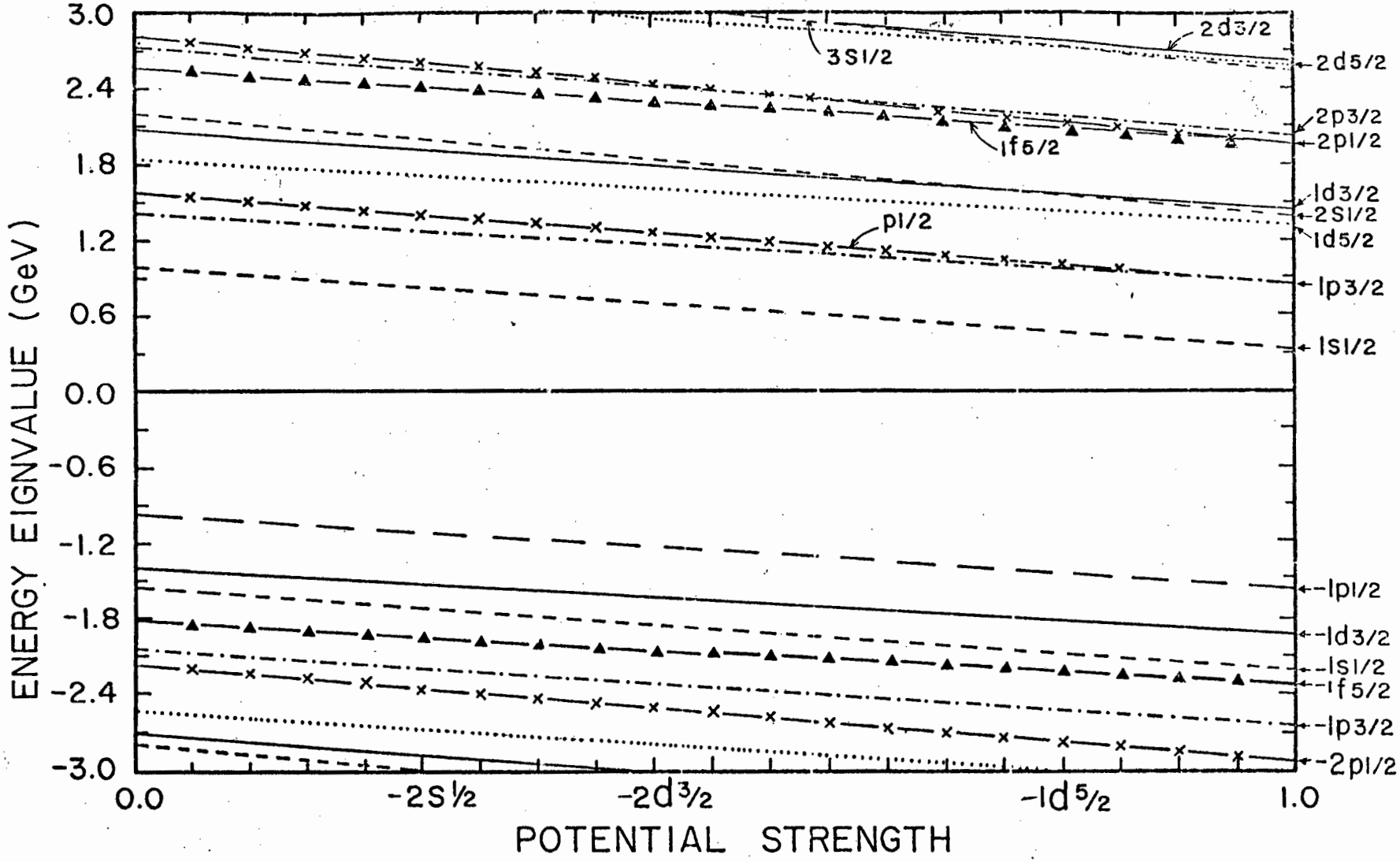

Figure 4.1 (b). The single particle energy for an antiquark of mass 0.3 GeV as a function of potential strength.

corresponds to the usual MIT bag model, the symmetry relation between positive and negative energy states

$$E(K,n) = -E(-K,-n) \qquad (4.1)$$

is recovered. Note that the splitting of consecutive radial excitations is also a function of the potential strength. The dependence of the spin-orbit splitting on the vector potential is quite noticeable from Figures 4.1(a) and (b). This is best illustrated by the $2p\,\frac{1}{2}$ and $2p\,\frac{3}{2}$ states for $m_q = 0.3$ GeV: in the absence of a vector potential the $p\,\frac{1}{2}$ state is higher in energy, but as the vector potential begins to dominate the scalar potential, the $p\,\frac{1}{2}$ state falls below the $p\,\frac{3}{2}$ in energy.

A comparison of Figure 4.1(a) and Figure 4.1(b) yields two observations about the effect of the quark mass on the energy eigenstates: firstly, that more massive states become more strongly bound in the potential; and secondly, that the splittings between the consecutive radial excitations are mass dependent too.

4.2 Meson masses

4.2.1 Model parameters

Experimental data on the masses of the scalar D^0 $(c\bar{u})$, D^+ $(c\bar{d})$, F^+ $(c\bar{s})$, B^- $(c\bar{u})$ and B^0 $(c\bar{d})$ particles and their spin-1 partners, the D^{0*}, D^{+*}, F^{+*} and B^{0*} are shown in Table 4.1. The mass of the B^{0*} has been inferred from the observation of

mono-energetic photons [18], believed to be produced in the decay

$$B^{0*} \rightarrow B^{0} + \gamma \quad .$$

	Meson masses (GeV)		
	Spin-0	Spin-1	cog
D^{+}	1869	2010	1973
D^{0}	1865	2010	1975
F^{+}	1970	2140	2098
B^{-}	5271	5325	5312
B^{0}	5274	5325	5313

Table 4.1 Meson masses as determined in experiment [19]

As the hyperfine interaction has not been taken into account, the mass of the centre of gravity of the D, F^{+}, B ($b\bar{u}$ or $b\bar{d}$) and as yet undiscovered $b\bar{s}$ (sometimes referred to as the E meson [20]) mesons has been calculated. The mass splitting between the D^{0} and D^{+} and the B^{0} and B^{+} due to electroweak interaction and a possible mass difference of the u and d quarks is ignored. The centre of gravity M_{cog} of the spin 1

mesons with mass M^*, and spin 0 mesons with mass M, is given by

$$M_{cog} = \frac{3M^* + M}{4} \quad . \qquad (4.2)$$

The up and down quarks are taken to be massless. $B^{1/4}$ is fixed as 145 MeV, this value being motivated from light quark spectroscopy [21]. The value of Λ, the mass scale parameter, is taken as 441 MeV on the basis of a non-relativistic modelling of the heavy quark bound states using the potential used in this model [22].

This leaves m_s, m_c and m_b, the masses of the strange, charmed and bottom quarks undetermined. These are fixed by fitting the masses of the mesons as determined by equations (3.1) and (3.2) to the centre of gravity of the experimental values of the meson masses.

The dependence of the groundstate energy of the antiquark (i.e. the difference between the meson mass and the mass of the heavy quark) is shown in Figure 4.2 as a function of the mass of the antiquark. This function must be known in order to fix the strange quark mass. The curve increases monotonically and shows no minimum, unlike the corresponding quantity $(E(\mu) + 2m)$ (μ is the reduced mass), obtained in a non-relativistic approach to the heavy quarkonium systems [23].

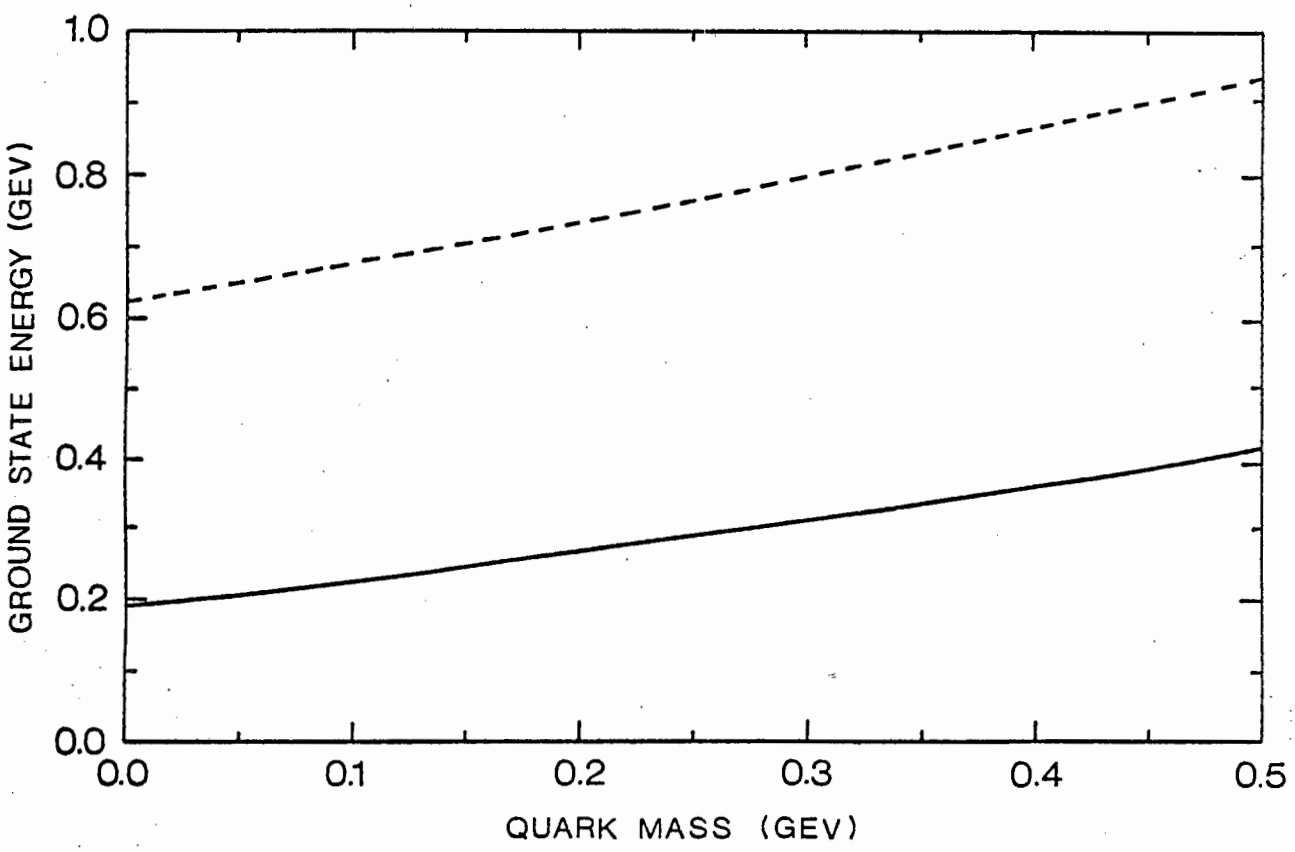

Figure 4.2 The groundstate energy of the light antiquark as a function of quark mass. The solid line indicates the relationship obtained with the exchange potential and the broken line the relationship with no exchange potential.

The values of the masses of the quarks used to obtain a fit and the resulting radius of the meson are shown in Table 4.2 as well as the prediction on the basis of this model for the E meson ($b\bar{s}$) mass. These values are shown alongside the values obtained using the MIT bag model without the additional exchange potential.

Parameters	Exchange potential	MIT
m_s	0.354	0.264
m_c	1.786	1.350
m_b	5.137	4.703
D,B radius	0.6875	0.8641
F,E radius	0.6829	0.8546
$m(E_{cog})$	5.437	5.437

Table 4.2 Quark masses required for fit and the corresponding meson radii. The masses are given in GeV, and the radii in fermi.

As expected, the introduction of the attractive Coulomb-like potential reduces both the energy of the light quark as well as the meson radius. A plot of $E(r_b)$ against r_b (see Figures 4.3(a) and 4.3(b) for m_q = 0 Gev and m_s = 0.3 Gev respectively) clearly shows the relation of the minima of the light antiquark's energy with respect to the bag radius in the presence or absence of the exchange potential.

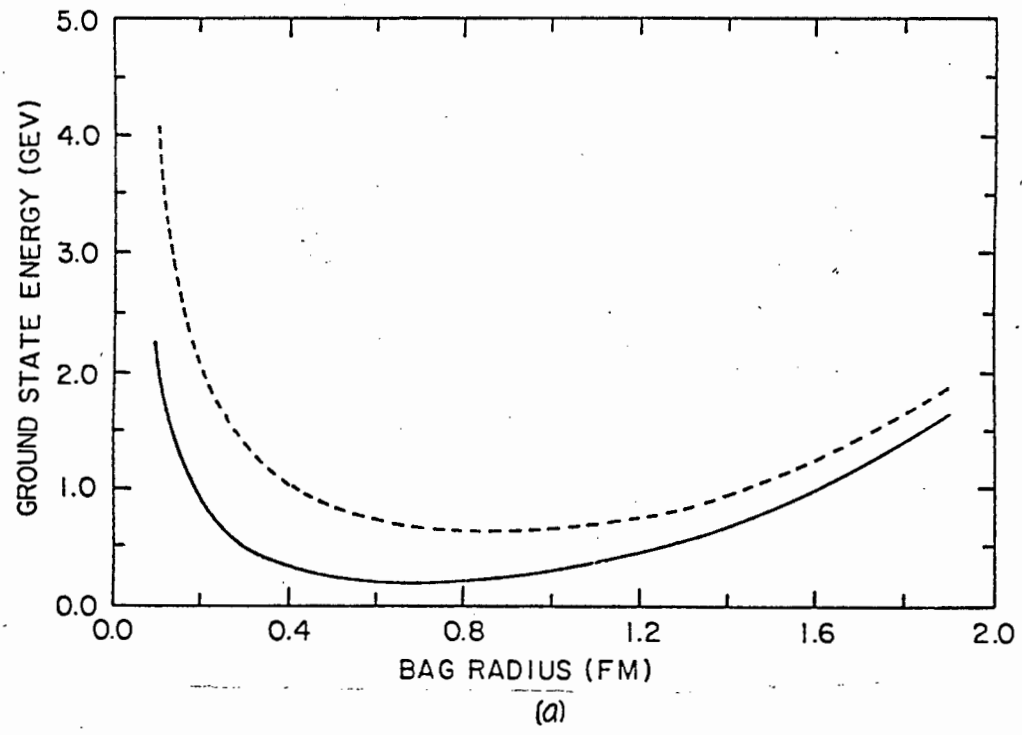

(a)

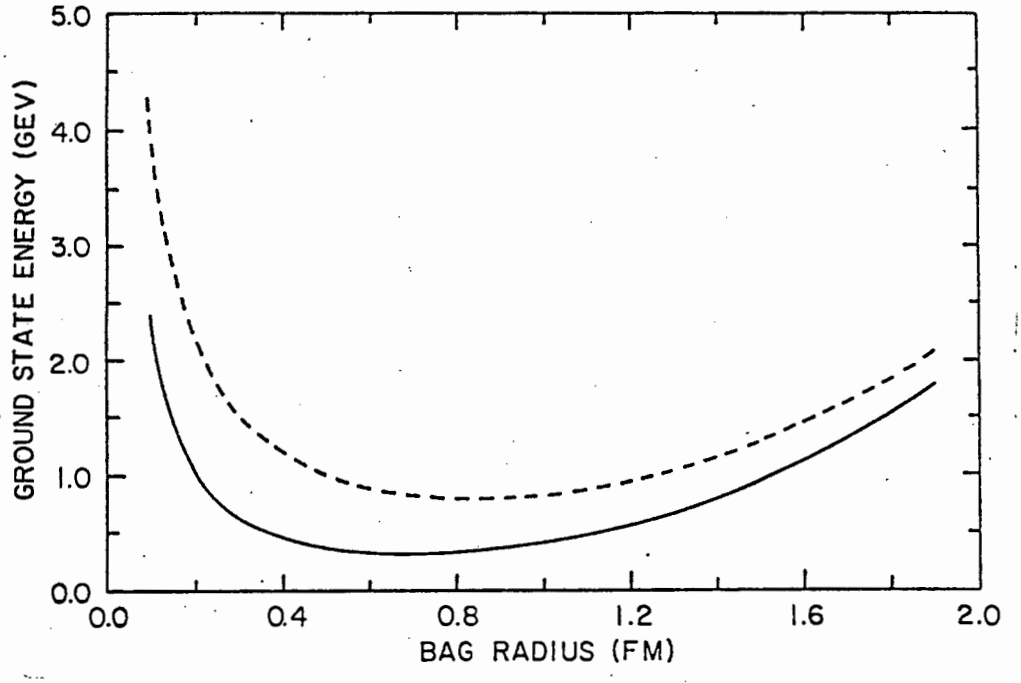

(b)

Figure 4.3. The groundstate energy of the light antiquark as a function of confinement radius in the presence (solid line) or absence (broken line) of the exchange potential for a massless antiquark (Figure (a)) and an antiquark of mass 0.3 GeV (Figure (b)).

4.2.2 The D, F, B and E spectra

The splitting between the radial and orbital excitations obtained in this model are shown in Table 4.3. along with the results of others (Eichten et al. [24], Crater and van Alstein [25]). Their results do not include spin-orbit interaction. The energies shown are given by the difference between the energy determined for the particular state and that obtained for the ground state. Ono [26] and Godfrey and Isgur [27] have also modelled the mesons, Ono concentrating on the hyperfine splitting of the ground states.

A general feature is the smaller splitting obtained between the energy levels in the relativistic models (this one, [25])than in the non-relativistic approaches ([24],[26]), with the splittings obtained in a non-relativistic treatment with relativistic corrections ([27]) falling somewhere in between.

	D,B	F,E		D^*	F^*	B^*	E^*	D	B
$1\ s\ \frac{1}{2}$	0	0	1 s	0	0	0	0	0	0
$1\ p\ \frac{1}{2}$	338	318	1 p	567	667	429	525	488	466
$1\ p\ \frac{3}{2}$	352	357							
$2\ s\ \frac{1}{2}$	624	558	2 s	585	583	519	525	753	707
$1\ d\ \frac{3}{2}$	688	632	1 d					866	819
$1\ d\ \frac{5}{2}$	715	612							
$2\ p\ \frac{1}{2}$	902	838	2 p					1107	1041
$2\ p\ \frac{3}{2}$	958	886							
$3\ s\ \frac{1}{2}$	1261		3 s					1339	1251

Table 4.3 $Q\bar{q}$ spectra. The first two columns give the results of this model, the spin-1 particle values are obtained in Ref. [25], while the spin-0 results come from Ref. [24]. Energies are given in MeV.

5. Summary and conclusion

Using a model which combines elements of the MIT bag model and relativistic potential models, the masses of the mesons consisting of a heavy quark and light antiquark have been evaluated. The calculation involves a relativistic treatment of the light antiquark moving in a static, spherically symmetric potential, with an inert heavy quark at the center.

Experimental data for the masses of the D, D^*, F, F^*, B and B^* mesons were used to fix the three parameters of this model - the masses of the strange, charmed and bottom quarks. This is unfortunately all the experimental data available which prevents the comparison of the predictions for the meson masses with experimental measurements.

However, the consistency of the values obtained for the masses of the charmed and bottom quarks can be checked by making use of some additional theoretical information on the hyperfine splitting.

The hyperfine splitting of the D and B quarks is due to the colourmagnetic moment of the quarks. The colourmagnetic moment of the heavy quark is inversely proportional to the mass. Thus in first order perturbation theory the hyperfine interaction scales as m_Q^{-1} [28]. Consequently the ratio of the hyperfine splittings of the D and B mesons is given by [29]

$$\frac{m(D^*) - m(D)}{m(B^*) - m(B)} = \frac{m_b}{m_c} \qquad (5.1)$$

From the values of the parameters obtained in this model and quoted in Chapter 4, one arrives at

$$m_b/m_c = 2.869 \qquad (5.2)$$

with the exchange potential, and without the exchange potential,

$$m_b/m_c = 3.473 \; . \qquad (5.3)$$

From (5.1) and the experimental data, one would expect a ratio of

$$m_b/m_c = 2.750 \; . \qquad (5.4)$$

Thus the quark mass ratio of this model is much closer to the best estimate given in (5.4) than the MIT bag value. This ratio appears to be fairly strongly model dependent and consequently perhaps provides the best means of testing the suitability of the the various models in view of the present lack of experimental data on the excited states of these mesons. In general, in non-relativistic models, a larger contribution to the mass of the meson comes from the antiquark, which leads to a much larger value for m_b/m_c than that given in (5.4).

To obtain the mass ratio quoted in (5.4) from this model, an interaction reducing the energy contribution from sources other than the mass of the heavy quark would be required. This interaction would have to reduce the energy by 0.121 GeV. The introduction of a negative self-energy of the antiquark or negative zero point energy term into this model could provide the neccessary energy reduction.

In fact, with the additional information available on the mass difference between the centre of gravity of the D meson and that of the B meson, one can obtain actual values for the masses of c and b. On the basis of equation (3.1) we have

$$m(B_{cog}) = m(D_{cog}) + (m_b - m_c). \qquad (5.5)$$

To satisfy both (5.1) and (5.5) the masses of the charmed and bottom quark should be 5.245 GeV and 1.907 GeV respectively. These values are far higher than those generally used in modelling these mesons as well as charmonium and bottomium. From this it appears that a strong quark-antiquark interaction is required to model these $Q\bar{q}$ systems consistently.

The splitting of the radially excited states and orbital excitations does depend on the potential used to describe the quark-antiquark interaction - when excited states of these mesons are discovered, more stringent checks of the type of interaction between the quark and antiquark will be possible. The success of a wide variety of potentials in reproducing experimental data on the charmonium and bottomiun systems is attributed to the fact that these systems probe only the range of these potentials where they are virtually indistinguishable [30]. In contrast, the successful modelling of the $Q\bar{q}$ systems using some kind of potential to account for the interaction will require a better understanding of this potential over another range.

Further insight into the validity of this approach could be obtained by investigating helium-like quark atoms - baryons

containing a heavy quark and two light quarks - modifying the potential by the necessary colour factor, each pair of quarks within a baryon necessarily being in a colour antitriplet state.

On another level, the computer programme developed could prove useful in other modelling procedures, in particular relativistic potential models which employ different (confining) potentials.

Acknowledgements

Many thanks go to my supervisor, Prof. R. D. Viollier, for all his guidance and time. I would like to express my gratitude to Prof. J. Rafelski for his advice and to Petr Zimak for much assistance, and am deeply indebted to Allard Schnabel for constant aid in battling The Computer. I sincerely appreciate Alice Kauffmann's assistance in the preparation of the illustrations. Thanks too to all the students inhabiting the nether corridors of the floor (especially the one who has shared a chaotic office with me for two years) for their moral(?) support

I am grateful to the CSIR for financial assistance in the form of a post graduate bursary.

Appendix A - Numerical methods and outline of computer programme

A FORTRAN programme was developed and executed on the APOLLO DN460 to find the energy eigenvalues of the light quark and then to minimise the contribution of the sum of this term and the volume energy term of the MIT bag model, both of which depend on the confinement radius.

A flowchart showing how the computer programme is structured is shown in Figure A.1. The details of the integration procedure are depicted in Figure A.2. The outline of the programme is as follows:-

(1) Calculate the exchange potential at points separated by one step-length and store these in an array.

(2) Having specified the value of the quark mass and confinement radius, divide the energy interval within which the energy eigenvalue is (hopefully) to be found into smaller divisions..

(3) For the first value of the energy, perform the numerical integration and evaluate the "Wronskian" (see Section A.4).

(4) Repeat the above for the next value of the energy. If the "Wronskian" has changed sign, use the root finding subroutine RZERO, a modified version of the CERN library programme C205 RZERO to obtain the energy for which the "Wronskian" vanishes.

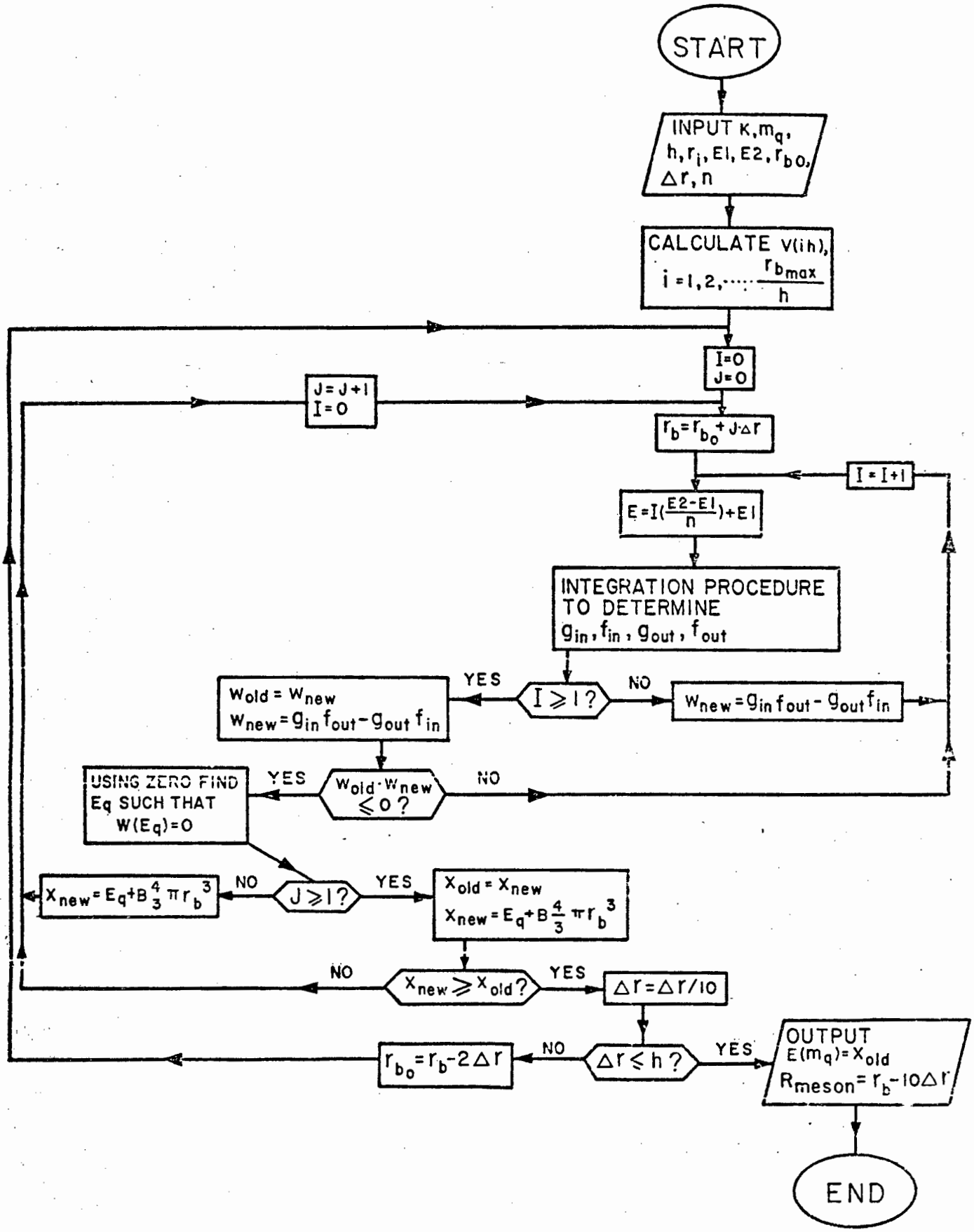

Figure A.1 Flowchart showing the computer programme structure

(5) Add the energy to the volume energy term and store the value.

(6) Repeat the procedure for the next value of the confinement radius.

(7) When the total energy is greater than the last, divide the interval between this confinement radius anc the one two before, into smaller intervals to pin down the minimum more accurately.

A.1 Numerical calculation of the exchange potential

The exchange potential V(r) is calculated at the discrete set of points $\{r_n\}$, $r_n = n.h$, where h is the step-length used in the integration of the wavefunction, $n = 1,2,\ldots r_{b\ max}/h$.

The expression for the exchange potential involves the integral

$$I = \int_0^\infty \frac{(1 - e^{-Mr})\ dM^2}{[(\log M^2/\Lambda^2)^2 + \pi^2]\ M^2} \qquad (A.1)$$

On change of variable to

$$t = \frac{1}{\pi} \arctan\left(\frac{1}{\pi} \log M^2/\Lambda^2\right) + \frac{1}{2} \qquad (A.2)$$

the integral (A.1) becomes

$$I = \int_0^1 1 - \exp\{-r\ \Lambda \exp[\frac{\pi}{2} \tan(\pi(t - \tfrac{1}{2}))]\}\ dt. \qquad (A.3)$$

This is then integrated using a 32-point Gauss integration procedure [31]:

$$I = \int_{-1}^{1} f(t)\, dt = \frac{1}{2} \sum_{i=1}^{32} w_i\, f(t_i) \qquad (A.4)$$

where $t_i = \frac{1}{2}(x_i + 1)$, (A.5)

with x_i the i^{th} zero of the Legendre polynomials $P_n(x)$, such that $P_n(1) = 1$,

and the weighting functions, w_i are given by

$$w_i = 2/(1 - x_i^2)\,[P_n'(x_i)]^2. \qquad (A.6)$$

A.2 Generating the initial values of the wavefunction

The initial values of the upper and lower component of the Dirac wavefunction are either Bessel functions of the first kind, or a linear combination of Hankl functions of purely imaginery argument.

The Bessel functions are calculated using the ascending series [32]

$$j_n(z) = \frac{z^n}{1.3.5...(2n+1)} \left\{1 - \frac{1/2\, z^2}{1!(2n+3)} + \frac{(1/2\, z^2)^2}{2!(2n+3)(2n+5)} - \ldots\right\} \qquad (A.7)$$

if $z < 2n + 1$.

If $z > 2n + 1$, the ascending series does not converge rapidly, so $j_n(z)$ is found using the recursion relation [33]

$$j_{n+1}(z) = \frac{2n+1}{z} j_n(z) - j_{n-1}(z) \qquad (A.8)$$

and defining

$$j_0(z) = \frac{\sin(z)}{z} \qquad (A.9)$$

and

$$j_1(z) = \frac{\sin(z)}{z^2} - \frac{\cos(z)}{z} \; . \qquad (A.10)$$

The Hankl functions of the first and second kind are generated using the series [34]

$$h_n^{(1)}(z) = i^{-n-1} z^{-1} e^{iz} \sum_{k=0}^{n} (n+1/2,k)(-2iz)^{-k} \qquad (A.11)$$

and $$h_n^{(2)}(z) = i^{n+1} z^{-1} e^{-iz} \sum_{k=0}^{n} (n+1/2,k)(2iz)^{-k} \qquad (A.12)$$

respectively,

where $$(n+1/2,k) = \frac{(n+k)!}{k!(n-k)!} \; . \qquad (A.13)$$

A.3 Numerical integration of the wave function

The equations determining the radial dependence of the upper and lower component of the Dirac wavefunction are two coupled first order differential equations,

$$\begin{pmatrix} g \\ f \end{pmatrix}' = \begin{bmatrix} \frac{K-1}{r} & -E + V(r) + m_q + S(r) \\ E - V(r) + m_q + S(r) & \frac{-K-1}{r} \end{bmatrix} \begin{pmatrix} g \\ f \end{pmatrix} \qquad (A.14)$$

and

These were solved using the Runge Kutta method which matches the Taylor expansion to four terms [35].

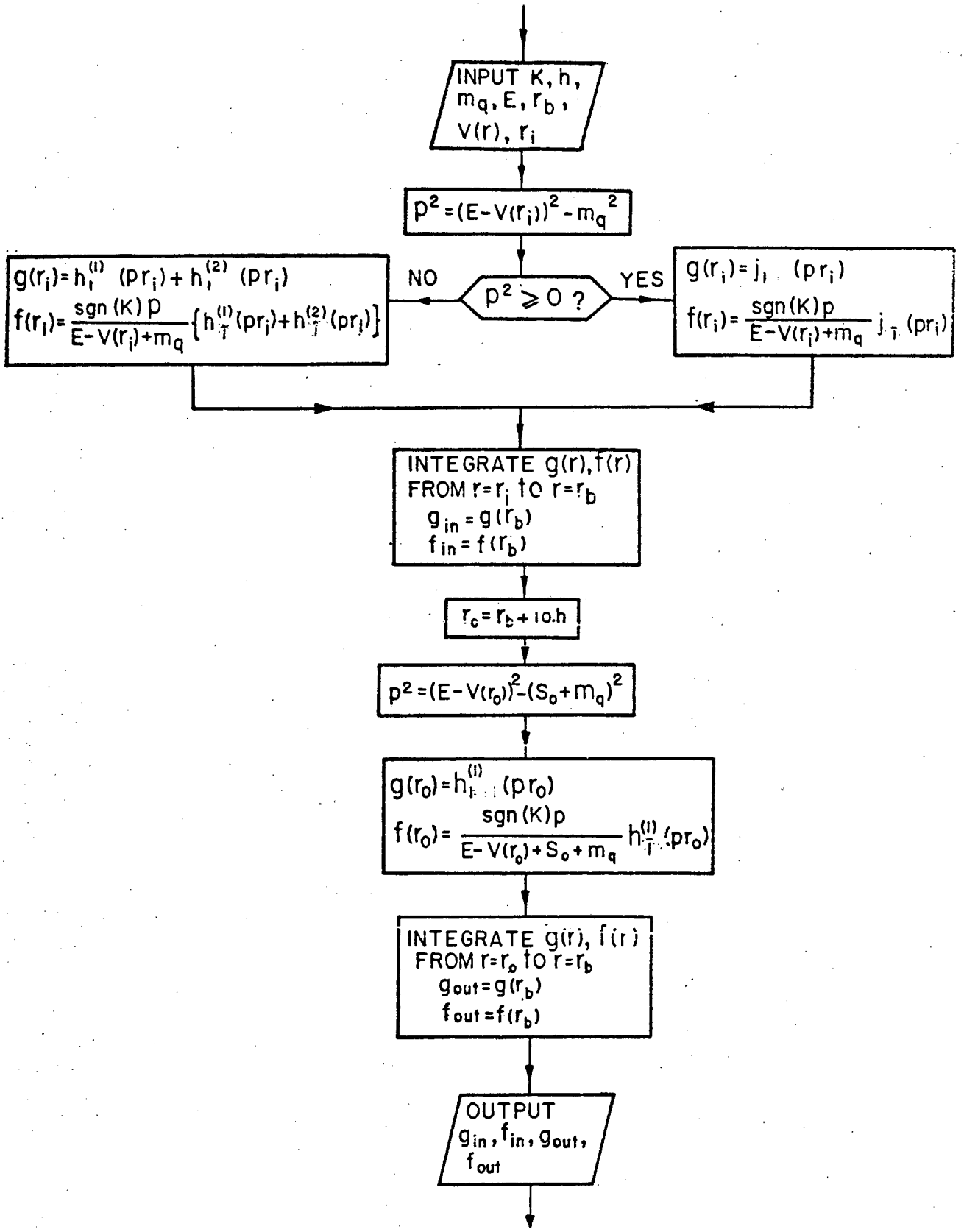

Figure A.2 Flowchart showing the details of the integration procedure.

Rewriting (A.14) as

$$\begin{pmatrix} g \\ f \end{pmatrix}' = \begin{bmatrix} A11 & A12 \\ A21 & A22 \end{bmatrix} \begin{pmatrix} g \\ f \end{pmatrix} \qquad (A.15)$$

the fourth order Runge Kutta method gives

$$g(r+h) = g(r) + \frac{1}{6}(k_1 + 2k_2 + 2k_3 + k_4) \qquad (A.16)$$

and

$$f(r+h) = f(r) + \frac{1}{6}(l_1 + 2l_2 + 2l_3 + l_4), \qquad (A.17)$$

where $k_1 = h\,(A11\ g(r) + A12\ f(r))$,

$l_1 = h\,(A21\ g(r) + A22\ f(r))$,

$k_2 = h\,[A11\ (g(r) + k_1/2) + A12\ (f(r) + l_1/2)]$,

$l_2 = h\,[A21\ (g(r) + k_1/2) + A22\ (f(r) + l_1/2)]$,

$k_3 = h\,[A11\ (g(r) + k_2/2) + A12\ (f(r) + l_2/2)]$,

$l_3 = h\,[A21\ (g(r) + k_2/2) + A22\ (g(r) + l_2/2)]$,

$k_4 = h\,[A11\ (g(r) + k_3) + A12\ (g(r) + l_3)]$

and $l_4 = h\,[A12\ (g(r) + k_3) + A22\ (f(r) + l_3)]$.

The integration is performed from r_i to r_b ($h > 0$), g_{in} and f_{in} are then the values of g and f respectively at r_b. From the integration from r_o towards r_b ($h < 0$), g_{out} and f_{out} are obtained as the values of g and f at the boundary.

A.4 Obtaining the energy eigenvalues

Defining the function $W(E,m_q,K,r_b)$

$$W(E,m_q,K,r_b) = f_{in}\, g_{out} - f_{out}\, g_{in} \qquad (A.18)$$

where f_{in} and g_{in} are the values of f and g respectively at r_b obtained from the numerical integration from the origin to $r = r_b$, and f_{out} and g_{out} are the values of f and g respectively at r_b obtained from the integration from $r > r_b$ to $r = r_b$, the energy eigenvalues of the possible bound states of the quark are those values of E (fixed m_q, K and r_b) for which $W(E,m_q,K,r_b)$ vanishes. This condition is equivalent to demanding the continuity of both the large and small component of the Dirac wavefunction.

The root of the function $W(E,m_q,K,r_b)$ is found using a modified version of the CERN library programme, C205 RZERO. This programme finds the root of a real valued function of one variable, in an interval within which the function changes sign. The root finding is based on the Muller method of parabolic interpolation supplemented by bisection.

A.5 Finding the minimum energy as a function of the confinement radius

The sum of the energy eigenvalue for the light quark and the volume energy term in the expression for the meson mass is calculated for successive values of the confinement radius r_b differing by Δr. After each calculation of the energy for a particular value of r_b, the result is compared with the value corresponding to the previous value of r_b. If this new value is greater than the last, the minimum must be located somewhere between the latest value of r_b, say r_l and $(r_l - 2\Delta r)$. Δr becomes $\Delta r/10$ and the process is repeated until $\Delta r < h$, the greatest degree of accuracy to which the position of the minimum can be found.

Appendix B: The linear boundary condition of the MIT bag model and the continuity of the Dirac wavefunction

The condition that both the large and small components of the Dirac wavefunction be continuous at all points, in particular at the bag boundary, is equivalent to the MIT bag boundary condition in the limit where the scalar step potential becomes infinite. This can be seen by examining the the ratios of the values of g and f outside the scalar well. From (3.15) and (3.16) this ratio is given by

$$\frac{g}{f} = \frac{h_l^{(1)}(pr)}{\frac{\mathrm{sgn}(K)\ p}{E_q - V + m_q + S}\, h_{\bar{l}}^{(1)}(pr)} \quad . \tag{B.1}$$

where

$$p^2 = (E_q - V)^2 - (m_q + S)^2 \quad . \tag{B.2}$$

Now
$$\frac{\mathrm{sgn}(K)\ p}{E_q - V + m_q + S} = \frac{\{(E_q - V(r) + m_q + S_0)(E_q - V(r) - m_q - S_0)\}^{1/2}}{(E - V(r) + m_q + S_0)}$$

$$= \frac{(E_q - V(r) - m_q - S_0)^{1/2}}{(E_q - V(r) + m_q + S_0)^{1/2}}\ \mathrm{sgn}(K)$$

$$\to (-1)^{1/2}\mathrm{sgn}(K) \qquad \text{as } S_0 \to \infty. \tag{B.3}$$

The ratio of the Hankl functions (see Appendix A, Section A.2) is given by

$$\frac{h^{(1)}_{l}(pr)}{h^{(1)}_{n}(pr)} = \frac{i^{-l}\sum_{k=0}^{l}\frac{(l+k)!}{k!(l-k)!}(2y)^{-k}}{i^{-n}\sum_{k=0}^{n}\frac{(n+k)!}{k!(n-k)!}(2y)^{-k}} \qquad (B.4)$$

where $y = -ipr$ and $n = \bar{l}$.

As $S_0 \to \infty$, $y \to \infty$ and only the $k = 0$ terms survive in expression (B.3). Thus

$$\lim_{S_0\to\infty} \frac{h^{(1)}_{l}(pr)}{h^{(1)}_{\bar{l}}(pr)} = -i\,\mathrm{sgn}(K) \; . \qquad (B.5)$$

Combining (B.3) and (B.4), outside the potential well, and consequently at the the confinement radius,

$$\frac{g}{f} = -1,$$

or $$g + f = 0 \qquad (B.6)$$

for an infinite scalar potential step.

(B.6) is just the linear bag boundary condition.

REFERENCES

1. James Joyce, Finnegan's Wake, London: Faber & Faber, 1939, p. 383.

2. R. D. Viollier and J. Rafelski, Helvetica Physica Acta **53** (1980), p. 352.

3. M. Gell-Mann, Phys. Lett. **8** (1964), pp. 214-216.

4. J. D. Bjorken and E. A. Paschos, Phys. Rev. 185 (1969), pp. 1975-1982.

5. O. W. Greenberg, Phys. Rev. Lett. **13** (1964), pp. 598 -602.

6. H. Fritzsch, M. Gell-Mann and H. Leutwyler, Phys. Lett. **B47** (1974), pp. 365-368.

7. A. Chodos, R. L. Jaffe, K. Johnson, C. B. Thorn, V. F. Weisskopf, Phys. Rev. **D9** (1974), pp.1094-1136.

8. E. Eichten, K. Gottfried, T. Kinoshita, K. D. Lane and T. M. Yan, Phys. Rev. **D21** (1980), p. 203.

9. J. L. Richardson, Phys. Lett. **82B** (1979), p. 272.

10. H. Crater and P. van Alstine, Phys. Lett. **100B** (1981), p. 166.

11. H. Pilkuhn, J. Phys. B: At. Mol. Phys. **17** (1984), pp. 4061-4080.

12. J. Rafelski and A. T. M. Aerts, private communication.

13. J. J. Sakurai, Advanced Quantum Mechanics, USA: Addison-Wesley Publishing Company, Inc., 1967, pp. 124-125.

14. R. D. Viollier and J. Rafelski, op. cit., p. 356.

15. Ibid., p. 358.

16. M. Brack, Phys. Rev. **D27** (1983), p. 1951.

17. W. A. Bardeen, M. S. Chanowitz, S. D. Drell, M. Weinstein and T. -M. Yan, Phys. Rev. **D11** (1975), pp.1106-1107.

18. K. Han et al., Phys. Rev. Lett. **55** (1985), p. 36.

19. Particle Data Group, Review of particle properties, (1982), pp. S203-S204.

20. E. Eichten, Phys. Rev. **D22** (1980), p. 1819.

21. T. De Grand, R. L. Jaffe, K. Johnson and J. Kiskis, Phys. Rev. **D12** (1975), p. 2070.

22. R. D. Viollier and J. Rafelski, op. cit., p. 358.

23. H. Crater and P. van Alstein, op. cit., p. 167.

24. E. Eichten, K. Gottfried, T. Kinoshita, K. D. Lane and T. M. Yan, op. cit., p. 230.

25. H. Crater and P. van Alstein, op. cit., pp. 170-171.

26. Seiji Ono, Phys. Rev. **D23** (1981), pp. 1118-1123.

27. E. Eichten and F. Feinberg, Phys. Rev. Lett. **43** (1979), p. 1207.

28. E. Eichten, op. cit., p. 1819.

29. Stephen Godfrey and Nathan Isgur, Phys. Rev. **D32** (1985), pp. 189-231.

30. A. Fridman, DESY preprint DESY 83-131 (1983), pp. 17-18.

31. M. Abramowitz and Irene A. Segun, eds., Handbook of Mathematical functions, USA: Dover Publications Inc., 1965, pp. 887-888.

32. Ibid., p. 437.

33. Ibid., p. 439.

34. Ibid., p. 439.

35. Ibid., p. 897.

BIBLIOGRAPHY

Abramowitz, Milton and Irene A. Segun, eds. Handbook of Mathematical Functions. USA: Dover Publications Inc. 1965.

Aerts, A. T. M. and J. Rafelski. Private communication.

Bardeen, W. A., M. S. Chanowitz, S. D. Drell, M. Weinstein and T.-M. Yan. "Heavy quarks and strong binding: A field theory of hadron structure". Physical Review D. Volume 11, Number 5. 1 March 1975. pp.1094-1136.

Bjorken, J. D. and E. A. Paschos. "Inelastic Electron-Proton and γ-Proton scattering and the Structure of the Nucleon". Physical Review. Volume 185, Number 5. 2 September 1969. pp. 1975-1982.

Brack,M. "Virial theorems for relativistic spin-$\frac{1}{2}$ and spin-0 particles". Physical Review D. Volume 27, Number 8. 15 April 1983. pp.1950-1953.

Chodos, A., R. L. Jaffe, K. Johnson, C. B. Thorn and V. F. Weisskopf. "New extended model of hadrons". Physics Review D. Volume 9, Number 12. 15 June 1974. pp.3471-3495.

Close, F. E. An Introduction to Quarks and Partons. London: Academic Press. 1979.

Crater, H. and P van Alstein. "Relativistic quark potential for the vector mesons". Physics Letters. Volume 100B, Number 2. 26 March 1981. pp. 166-172.

De Grand, T., R. L. Jaffe, K. Johnson and J. Kiskis. "Masses and other parameters of the light hadrons". Physical review D. Volume 12, Number 7. 1 October 1975. pp. 2060-2076.

De Tar, Carlton E. and John F. Donoghue. "Bag models of hadrons". Annual Review of Nuclear and Particle Science. Volume 33. 1983. pp.235-264.

Eichten, E. "Υ family of resonances above threshold". Physical Review D. Volume 22, Number 7. 1 October 1980. pp. 1819-1823.

Eichten, E. and F. Feinberg. "Spin-dependent forces in Heavy Quark Systems". Physical Review Letters. Volume 43, Number 17. 22 October 1979. pp. 1205-1208.

Eichten, E., K. Gottfried, T. Kinoshita, K. D. Lane and T. M. Yan. "Charmonium: Comparison with experiment". Physical Review D. Volume 21, Number 1. 1 January 1980. pp. 203-233.

Eggers, Hans Christoph. Meson spectra using relativistic quark models. Master's Thesis. Unpublished.

Fridman, A. "Introduction to Quarkonium Physics". DESY preprint DESY 83-131. December 1983.

Fritzch, H., M. Gell-Mann and H. Leutwyler. "Advantages of the color octet gluon picture". Physics Letters. Volume 47B, Number 4. 26 November 1973. pp. 365-368.

Gell-Mann, M. "A schematic model of baryons and mesons". Physics Letters. Volume 8, Number 3. 1 February 1964. pp. 214-216.

Godfrey, Stephen and Nathan Isgur. "Mesons in a relativized quark model with chromodynamics." Physical Review D. Volume 32, Number 1. 1 July 1975. pp. 189-231.

Greenberg, O. W. "Spin and unitary-spin independence in a paraquark model of baryons and mesons". Physical Review Letters. Volume 13, Number 20. 16 November 1964. pp. 598-602.

Halzen, Francis and Alan D. Martin. Quarks and Leptons: An Introductory Course in Modern Particle Physics. USA: John Wiley and Sons. 1984.

Han, K. et al. "Observation of B^{*} Production in $e^{+}e^{-}$ Interactions above the b-Flavor Threshold". Physical Review Letters. Volume 55, Number 1. 15 July 1985. pp. 36-40.

Huang, Kerson. Quarks Leptons and Gauge Fields. Singapore: World Scientific Publishing Co Pte Ltd. 1982

Joyce, James. Finnegan's Wake. London: Faber & Faber. 1939.

Lee, T. D. Particle Physics and Introduction to Field Theory. USA: Harwood Academic Publishers. 1981.

Martin, A. "Flavour Independence of Forces Between Quarks". TH.2741-CERN. 18 September 1979.

Ono, Seiji. "Strong decay widths of $b\bar{b}$ states above threshold". Physical review D. Volume 23, Number 5. 1 March 1981. pp. 1118-1123.

Particle Data Group. Review of Particle Properties. USA: American Physical Society. April 1982.

Pilkuhn, H. "Spinor equations for binary atoms". Journal of Physics B: Atomic and Molecular Physics. 17 (1984). pp4061-4080.

Quigg, Chris. Gauge Theories of the Strong, Weak, and Electromagnetic Interactions. USA: The Benjamin/Cummings Publishing Company, Inc. 1983.

Richardson, J. L. "The heavy quark potential and the Υ, J/Ψ systems". Physics Letters. Volume 82B, Number 2. 26 March 1979. pp. 272-277.

Sakurai, J. J. Advanced Quantum Mechanics. USA: Addison-Wesley Publishing Company, Inc. 1967.

Viollier, R. D. and J. Rafelski. "Quarkonium spectra in the framework of Quantum Chromodynamics". Helvetica Physica Acta. Vol. 53 (1980). pp.352-368.

Yndurain, F. J. Quantum Chromodynamics An Introduction to the Theory of Quarks and Gluons. New York: Springer-Verlag. 1983.

Zimak, Petr. Das $q^2\bar{q}^2$ - System im Rahmen des MIT Bagmoddels. Diploma thesis. Unpublished.